Diagnostic Radiology in Hematological Patients with Febrile Neutropenia

7

Claus Peter Heussel

Contents

C.P. Heussel
Diagnostic and Interventional Radiology, Chest Clinics at University Hospital Heidelberg, Amalienstrasse 5, Heidelberg 69126, Germany
e-mail: heussel@uni-heidelberg.de

7.1   Early Detection of Pneumonia

The necessity for early detection of the focus of infection is based upon high fatality of infections in immunocompromised hosts, increasing within hours of delayed appropriate treatment [48]. (This paper does not refer to immunocompromised patients; maybe Greene 2007 [52] or Cornely 2010 [58] could be used), a potential negative impact of delayed diagnosis (i.e., more advanced infection) on future antineoplastic treatment, and high costs of prolonged hospitalization. This has to be compared with the costs of a non-enhanced CT scan, which is around € 230 in German hospitals. After physical examination and interpretation of laboratory findings, the search for an infectious focus starts with the identification of the most suspected organ system(s). The appropriate imaging technique has to be selected demanding for high sensitivity and clinically meaningful negative predictive value [4].

Exact proportions of organ involvement are difficult to determine and may differ from clinical and pathological findings, the latter often obtained from autopsies (i.e., negative selection). Clinically, lungs are affected in 30 % of febrile neutropenic patients and allogeneic hematopoietic stem cell transplant (aSCT) recipients, paranasal sinuses in 3 % of neutropenic patients, and 30 % in the aSCT setting (concomitant to pneumonia), while the gastrointestinal tract, liver, spleen, central nervous system, and kidneys are less frequently involved [4].

7.1.1   Conventional Chest Radiograph

Chest x-ray (CXR) is still frequently used when pneumonia is suspected or should be ruled out [14, 15]. CXR has several advantages: it is quick, widely available (even on the ward), inexpensive, and associated with a low radiation dose. CXR is occasionally done on the ward to keep neutropenic patients in protective isolation, even if performed in supine position. But CXR has the crucial disadvantage of superimposition and therefore a very limited sensitivity for the detection of pneumonia (Figs. 7.2 and 7.6) [14, 16]. Especially if performed in supine position, lung inflation is worse and lateral projection is lacking, which limits image quality besides other technical issues. In patients with fever of unknown origin (FUO) after SCT, digital CXR in supine position achieves a sensitivity for early detection of pneumonia of only 46 % [17]. While CXR provides relevant clinical information concerning central venous catheters (CVC), pleural effusion, and pulmonary congestion [17], it fails to enable early detection or exclusion of pneumonia, which is a major task in immunocompromised hosts. CXR in supine position alone is therefore not recommended for the early detection of pneumonia in these patients [5]. Also, if an infiltrate is apparent at CXR, the options for its characterization are very limited. If pneumonia is considered in these hosts, thin-section CT should be preferred at any time [18].

7.1.2   CT Technique and Terminology

The radiation dose is of limited concern in patients who eventually underwent local or total body irradiation and received cytotoxic agents, etc., considering that actual CT techniques apply 1–10 mSv per lung scan (in this diagnostic scenario: mSv = mGy) [19, 20]. The risk of developing a radiation-induced neoplasm, even after several diagnostic exposures, is low when compared to the high mortality associated to infection and disease as well as the risk of a secondary malignancy due to anti-neoplastic treatment.

Terms like *incremental CT*, *high-resolution CT* (HRCT), *spiral CT*, *thin-section CT*, *multislice CT* (MSCT), and *low-dose CT* are widely used and might confuse non-radiologists. To keep it simple, HRCT is an incremental scanning technique with several respiratory breath-holds resulting in inaccuracy of repositioning of the anatomical lung position. The use of 1 mm sections and gaps in between (e.g., 10 mm) results in representative, detailed images of selected lung areas; however, the noncontiguous scanning has its limitations in nodule detection, quantification, and monitoring. Volumetric techniques as used in spiral CT and MSCT, acquired without gaps, are frequently reconstructed with larger thickness (e.g., 5 mm) resulting in spatial volume effects. This results in limitations to detect inflammatory lung disease, especially ground-glass opacification [22]. Since no additional information is expected from supplemental spiral CT to HRCT, as shown in AIDS patients [23], HRCT may be used as a diagnostic standard. In contrast, thin-section MSCT provides volumetric scanning as well as detailed images [24, 25]. This technique also allows for an adequate monitoring of lung disease since the same anatomical position can be reidentified in baseline and follow-up studies [24–26]. While a rapid technical development in CT imaging is ongoing, the different techniques applied today are addressed as "CT" in this chapter.

In general, contrast enhancement is not required for detecting and characterizing pneumonia [6, 18]. Only in special situations such as suspicion of pulmonary embolism or hemoptysis caused by vessel erosion is CT angiography beneficial (Fig. 7.1) [27]. In the aSCT setting, bronchiolitis obliterans is to be considered [24, 28] where air-trapping is a relevant finding. Here, an additional expiratory CT scan is helpful [24, 28].

7.1.3   CT

The advantage of HRCT in comparison to CXR for the early detection of pneumonia was demonstrated in febrile neutropenic patients not responding to empirical antibiotic therapy [21]. In approximately 60 % of the patients with a normal CXR, HRCT showed pulmonary infiltrates (Fig. 7.2). In only 10 % of patients with a normal chest x-ray and a normal HRCT, pneumonia occurred during follow-up [21]. Exclusion of pneumonia is another clinically relevant information. Thus, CT yields
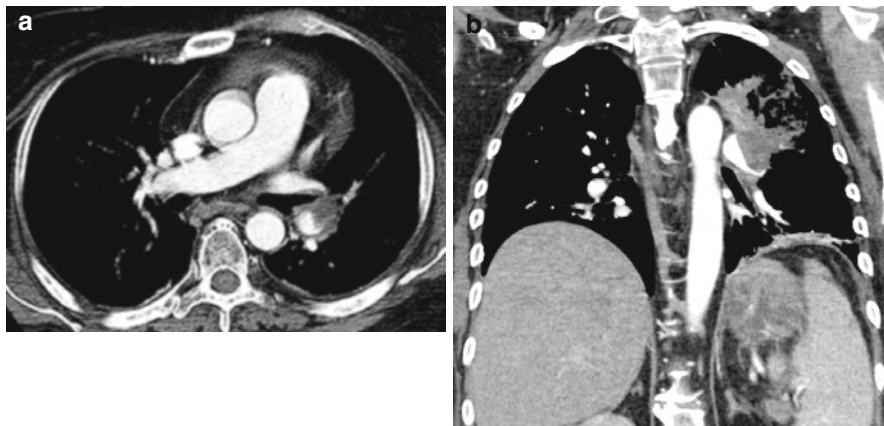
Fig. 7.1 Contract-enhanced CT demonstrates vessel erosion in a consolidating infiltrate of the left lung. An apposition thrombus can be depicted in the pulmonary artery of the left lower lobe of this 45-year-old female who underwent unrelated PBST 6 months before due to AML. She died 2 days later from brain infarction

very useful results with good sensitivity (87 %) and negative predictive value (88 %). The early use of HRCT achieves a gain of approximately 5 days during which pneumonia may be excluded [17]. In clinical practice, this may be very helpful for the management of immunocompromised hosts at high risk of life-threatening pulmonary infection [5] (Fig. 7.2).

7.1.4 Magnetic-Resonance Tomography (MRI)

MRI has been evaluated for the investigation of pulmonary disease since it has a known benefit in lesion characterization [29, 30]. Comparing CT to MRI on an intraindividual basis, MRI reveals comparable clinical results (sensitivity 95 %, specificity 88 %, positive predictive value 95 %, negative predictive value 88 %) [53]. Besides the lack of radiation, there is no clear advantage of MRI in the early detection of pneumonia (Fig. 7.3). In advanced stages, CT and MRI are comparable in the visualization of infiltrates [30]. CT is widely available, easier, and faster to perform as well as less susceptible to breathing artifacts. MRI is superior to CT in the detection of abscesses due to a clearer detection of central necrosis in T2-weighted images and rim enhancement after contrast application in T1-weighted images [29]. However, this fact has limited clinical impact and duration of MRI, and required compliance is substantially higher compared to CT. MR has problems to detect small lesions and those which are adjacent to the left ventricle due to the cardiac motion [53].
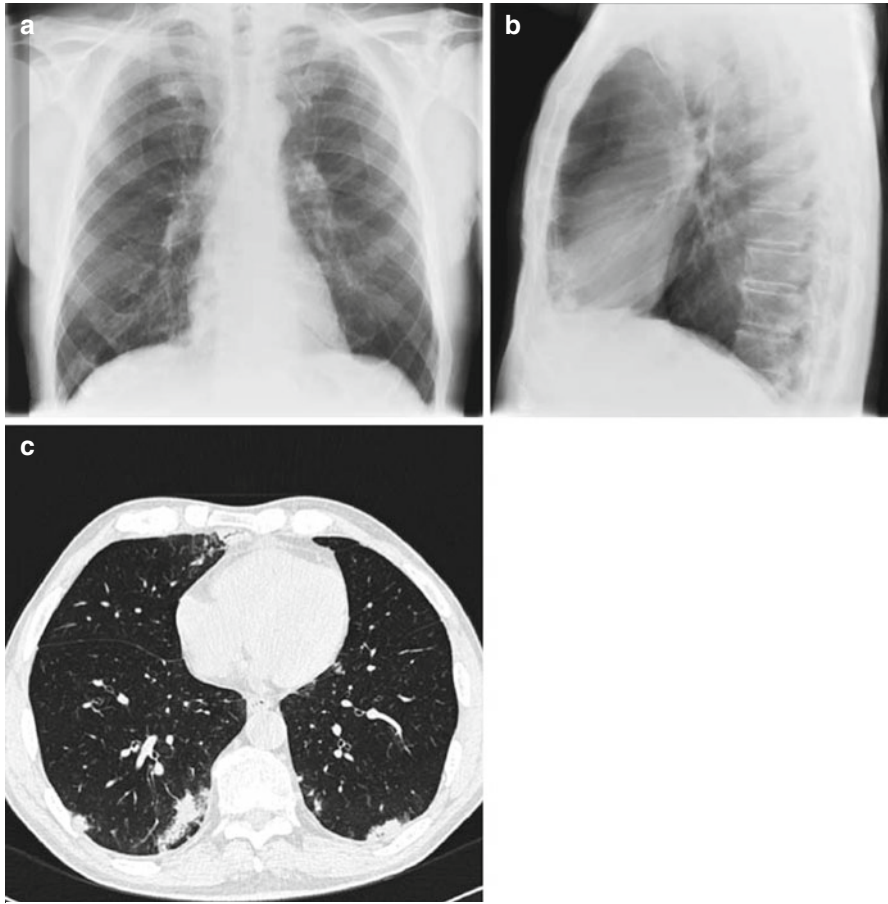
Fig. 7.2 Neutropenic febrile patient receiving broad-spectrum antibiotic therapy. CXR was normal at day 3 of fever (**a**, **b**). HRCT performed the same day demonstrates bilateral infiltrates, which were hidden behind the heart in posterior-anterior and the spine in lateral projection (**c**)

7.1.5   Recommendation for Clinical Practice

In contrast to systemic infections, identification of the underlying organism in pneumonia is more difficult and complex. Attempts to reinforce pathogen identification did not improve the clinical outcome significantly [9]. Therefore, a calculated (preemptive) decision on antimicrobial therapy in febrile immunosuppressed patients based on imaging studies is widely used.

The use of CT is recommended for the early detection of pneumonia [9]. It may serve for indication and localization of invasive diagnostic procedures such as
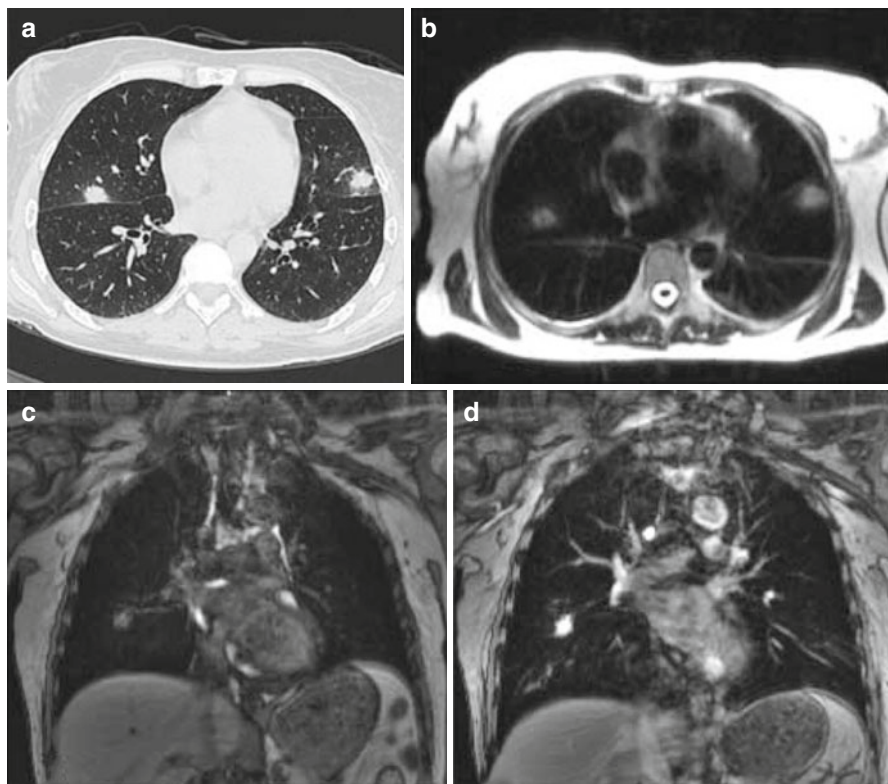
**Fig. 7.3** Fungal pneumonia in HRCT (**a**), T2-weighted (**b**), non-enhanced T1-weighted GE MRI (**c**) and after Gd application performed the same day (**d**). Lesion contrast is similar in CT and contrast-enhanced MRI

bronchoscopy and bronchoalveolar lavage or CT-guided biopsy. On the other hand, the exclusion of pneumonia can be obtained with a higher reliability as compared to conventional CXR. The sequential cascade as shown in Fig. 7.4 can be modified if the local institutional CT capacity allows for the skipping of CXR.

7.2 Monitoring of Lung Infiltrates

An increasing size of pulmonary infiltrates during hematopoietic recovery has been well described by [31]. Caillot et al. evaluated HRCT in neutropenic patients with proven pulmonary aspergillosis at weekly intervals [31] and documented the time points of different radiological patterns and evaluated the size of infiltrates and documented the time points of different radiological patterns and evaluated the size of infiltrates. They frequently found a "halo sign" (Fig. 7.5) on the first CT scans and reported a low sensitivity of this pattern (68 %), which was no longer visible on follow-up scans. In contrast, the more specific "air-crescent sign" (Fig. 7.7) emerged
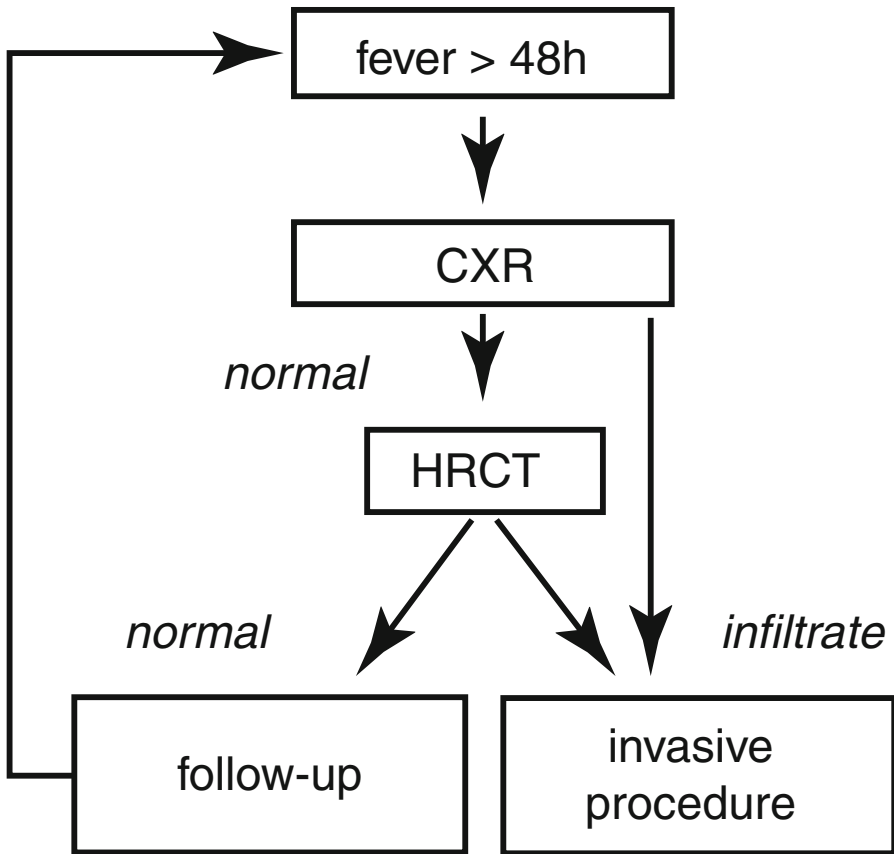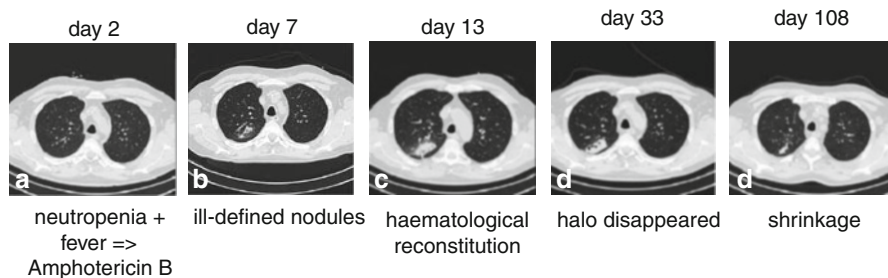
Fig. 7.4 Recommendations of the Guidelines of the Infectious Diseases Working Party (AGIHO) of the German Society of Hematology and Oncology (DGHO) [13]. Since the initial CXR is of limited use, this diagnostic step is more and more omitted and CT is performed primarily

frequently during follow-up (up to 63 %). The size of infiltrates increased by fourfold under successful antifungal treatment due to hematopoietic reconstitution. In this study, pneumonia was first detected on day 19 of neutropenia. Enlargement of infiltrates is probably caused by the invasion of newly generated neutrophil granulocytes at the beginning of bone marrow recovery. In critically ill patients, leukocyte invasion has been described as a risk factor for the development of acute respiratory distress syndrome (ARDS) [14] (Fig. 7.6 and 7.7).

7.3   Characterization of Pneumonia

Radiologists' dream is to be capable to identify the underlying microorganism in pneumonia of immunocompromised hosts with a sufficient specificity. In some cases, imaging can provide very fast useful hints, but no verification. The quality of these clues

day 2	day 7	day 13	day 33	day 108

neutropenia + fever => Amphotericin B | ill-defined nodules | haematological reconstitution | halo disappeared | shrinkage

Fig. 7.5 Neutropenic febrile patient who underwent autologous peripheral blood stem cell transplantation. On day 2 after posttransplant, empirical mold-active antifungal treatment was started for neutropenic fever. Ill-defined pulmonary nodules were detected on day 7. Due to marrow recovery on day 13, the volume of lung infiltrates reached its maximum. Under continued antifungal treatment, the halo slowly disappeared and a central cavitation developed (day 33). The lesions shrinked significantly until day 108

depends on the cooperation between clinicians and radiologists and on the radiologists' experience with these complications. This requires an informational exchange concerning relevant individual patient data like severe neutropenia or allogeneic stem cell transplantation. For example, information on reactivation of cytomegalovirus (CMV) in a patient with graft-versus-host disease is very helpful for the correct interpretation of pulmonary HRCT findings. Also the chemotherapy or total body irradiation applied for conditioning before aSCT may be relevant for differential diagnostic considerations in patients who might present with clinically similar signs and symptoms [6, 7, 32, 33]. Some of the most useful clues are listed in Table 7.1.

7.3.1 Bacterial Pneumonia

Bacteria are causing approximately 90 % of infections during the early phase of neutropenia [8]. The radiological appearance of bacterial pneumonia includes consolidation, especially bronchopneumonia and positive pneumobronchogram (Fig. 7.2) [33, 34]. In contrast to immunocompetent patients, ground-glass opacification is found more often and remains nonspecific.

7.3.2 Fungal Pneumonia

Severe neutropenia lasting for more than 10–14 days is associated with an increasing risk of invasive fungal infection [3], with *Aspergillus species* being the primary pathogen, while *Candida species* very rarely cause primary pneumonia (Fig. 7.8) [5]. Typical radiological findings of fungal and non-fungal pneumonia as
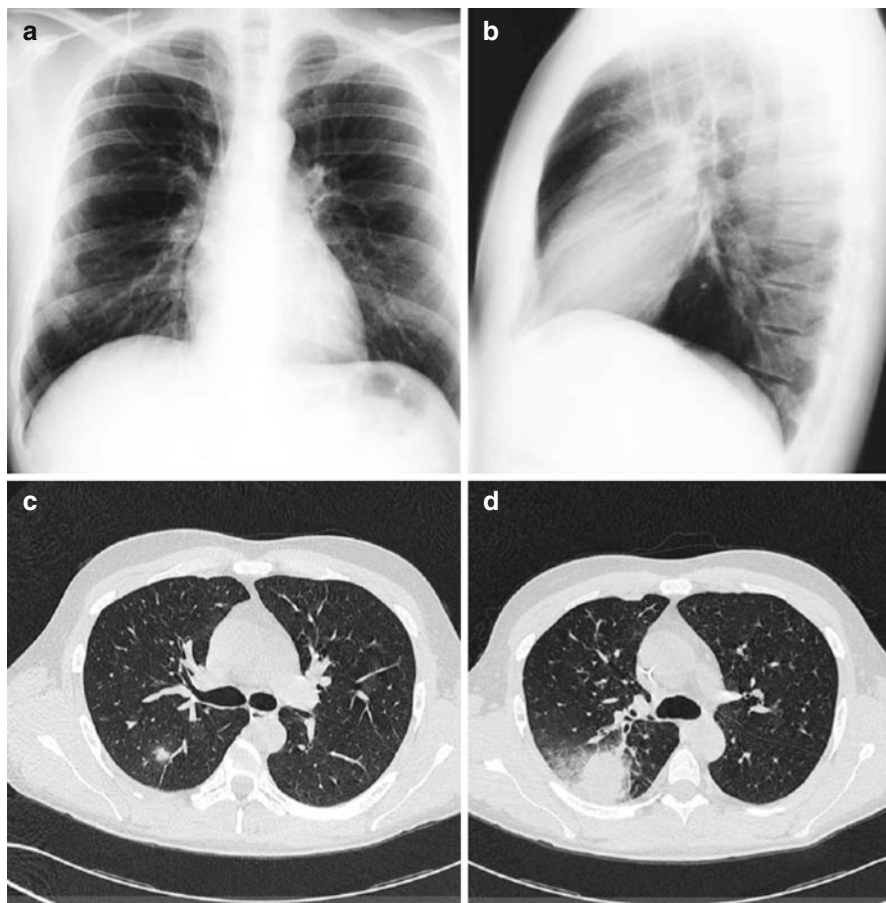
Fig. 7.6 The small ill-defined nodule in the right upper lobe (**c**) of this 34-year-old neutropenic AML patient was even retrospectively not visible on conventional chest x-ray done at the same day (**a**, **b**). Amphotericin B treatment was started due to suspicion of fungal pneumonia; however, the nodule size increased during hematopoietic reconstitution 2 weeks later (**d**). In preparation of bone marrow transplantation, the lesion was surgically resected and *Aspergillus* pneumonia was verified

well as of infiltrates from noninfectious diseases have been reviewed in detail [35]. The typical appearance of pulmonary infiltrates from fungal origin are as follows:

Early phase of fungal pneumonia:	Ill-defined nodules (Figs. 7.3, 7.5 and 7.8) [33] in combination with the Halo sign (Figs. 7.5 and 7.8) [33], which is nonspecific
Late phase:	Air-crescent sign [36]
	Cavitation (Fig. 7.8)

Fig. 7.7 Non-fungal lung infiltrate: ill-defined nodules with cavitation on CT scans done due to repeated febrile episodes. They appeared like fungal pneumonia and were not visible on baseline CT. After removal of a central venous port system, both the pulmonary lesions as well as the febrile episodes, disappeared
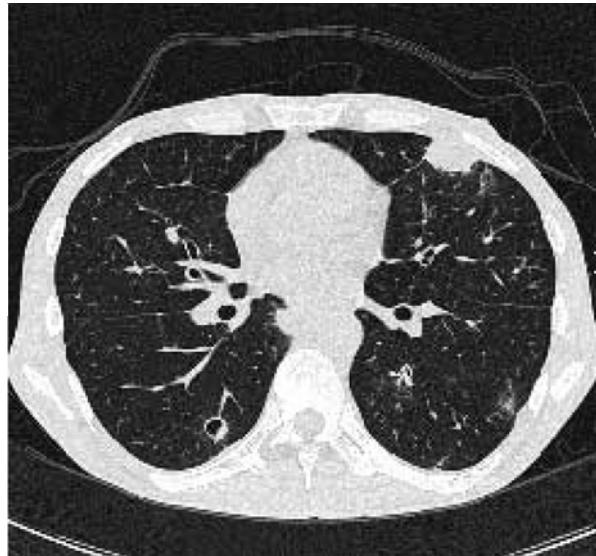
For use in the context of clinical and epidemiological research in neutropenic patients, standards for the interpretation of radiological findings in invasive fungal infections have been elaborated [10, 51]; newly emerged "typical" CT patterns (dense, well-circumscribed lesions with or without a halo sign, air-crescent sign) are classified as a clinical criterion for fungal pneumonia Figs. 7.5 and 7.8. The halo sign, first described in 1984 [49, 50], is nonspecific [33] and not a necessary part of the updated definitions [51]. A nonspecific infiltrate, rated as a minor criterion in the first version [10], was abandoned in the update [51]. In a later workup of a pharmaceutical trial investigating response rates to antifungal treatment, the evidence of the halo sign was associated with an improved response rate (52 % vs. 29 %; $p < 0.001$), as well as a higher 3-month survival rate (71 % vs. 53 %; $p < 0.01$) [52]. This large ($n = 235$) antemortem trial suffers, however, from systemic limitations like investigation of halo which was part of inclusion criteria and technical insufficiencies like usage of thick-section CT instead of appropriate thin-section CT and evaluation of hardcopies instead of monitor reading [52]. Histopathological workup of lung biopsies verified fungal pneumonia in 56 % of cases in another study [37]. Relevant differential diagnoses for the halo sign, such as cryptogenic organizing pneumonia (COP, formerly known as bronchiolitis obliterans organizing pneumonia, BOOP), pulmonary hemorrhage, pulmonary manifestation of the underlying malignancy, lung cancer, and non-fungal infections (CMV, tuberculosis, abscesses (Fig. 7.7), etc.) or *Candida* (Fig. 7.8), have to be considered [37].

Thus, diagnostic clarification will frequently be necessary, particularly when antifungal treatment is not successful.

Table 7.1 Clinical and radiological appearance for various infectious and noninfections lung abnormalities in neutropenic hosts and after allogeneic stem cell transplantation

Diagnosis	Clinical setting	Radiological appearance
Infection bacterial	Early phase neutropenia	Consolidation, bronchopneumonia positive pneumobronchogram, GGO
Fungal	Long-term neutropenia (>10 days)	Halo = ill-defined nodules (early phase)
		Consolidations negative pneumobronchogram
		Air-crescent sign/cavitation (late phase)
Pneumocystis	Allogeneic transplantation	GGO, spared-out subpleural space
		Intralobular septae (late phase)
Tuberculosis	Each	Small ill-defined nodules/cavitations, tree in bud, homogeneous consolidation
Viral	Transplant history in graft or host	GGO – mosaic pattern
Graft versus host	Allogeneic transplantation	GGO – mosaic pattern
		Intralobular septae become visible
		Tree in bud
		Air-trapping (expiratory CT)
Radiation toxicity	Total body irradiation	GGO – paramediastinal distribution, also after TBI
		Intralobular septae become visible
Drug toxicity	Bleomycin, methotrexate, high-dose cytarabine, carmustine, etc.	GGO – mosaic pattern
		Intralobular septae become visible
		Peripheral consolidations of secondary lobule
		Traction bronchiectasis
Pulmonary congestion	Extensive hydration, renal impairment, hypoproteinosis	GGO
		Interlobular septae become visible
Leukemic infiltration	Pulmonary involvement	Thickening bronchovascular bundles thickening
		Interlobular septae become visible
		GGO
Pulmonary hemorrhage	Thrombocytopenia, post-interventional, hemoptysis	GGO – sedimentation phenomenon

GGO ground-glass opacification, *TBI* total body irradiation

Air-crescent sign and cavitation occur with hematopoietic reconstitution during the late phase of fungal infection (Fig. 7.8) [36]. Both radiological signs are known to be associated with a favorable prognosis. However, the specificities of these findings are limited, and relevant differential diagnoses have to be considered (Fig. 7.7) [37]. There are other useful patterns for the identification of fungal pneumonia, e.g.,
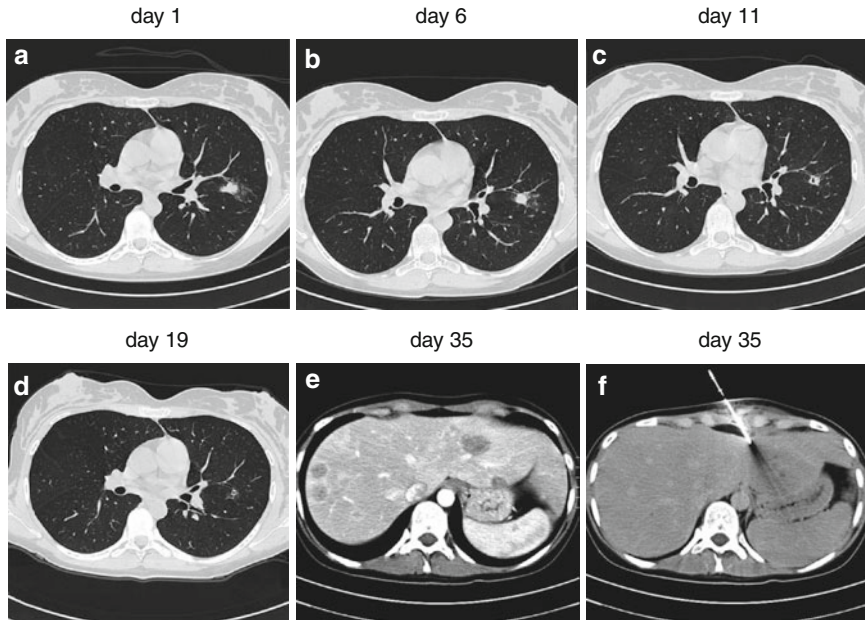
Fig. 7.8 Bilateral ill-defined nodules prompted the suspect of a fungal infection which was treated accordingly. *Candida* spp. were isolated from blood culture. Due to increasing liver enzymes, contrast-enhanced CT scan of the liver was ordered. Biopsy from the detected lesions confirmed *Candida* spp.

distribution along the bronchovascular bundle resulting in the feeding vessel sign with an angiotrophic location.

The ongoing development of antifungal therapy may have an important impact on the radiological appearance of fungal pneumonia. Thus, in the near future radiologists will not only be confronted with the question for "breakthrough fungal pneumonia," but also for fungal pneumonia caused by non-*Aspergillus* pathogens.

7.3.3 *Pneumocystis jiroveci* Pneumonia (PcP)

Pneumocystis jiroveci pneumonia (PcP) [38] is a typical finding in hematological patients affected by severe cellular (T-cell) immunosuppression and those with graft-versus-host disease after aSCT, if they are not protected by effective chemoprophylaxis [8]. Despite standard trimethoprim-sulfamethoxazole prophylaxis, 8 % of the patients develop PcP, while among patients without prophylaxis, the incidence may reach 29 % [8]. Up to 15 % of these patients will have a fatal outcome [8].

CT provides a valuable characterization for PcP [6, 7, 18, 33] and is a reliable method for discriminating it from other infectious processes [33, 39]. A combination
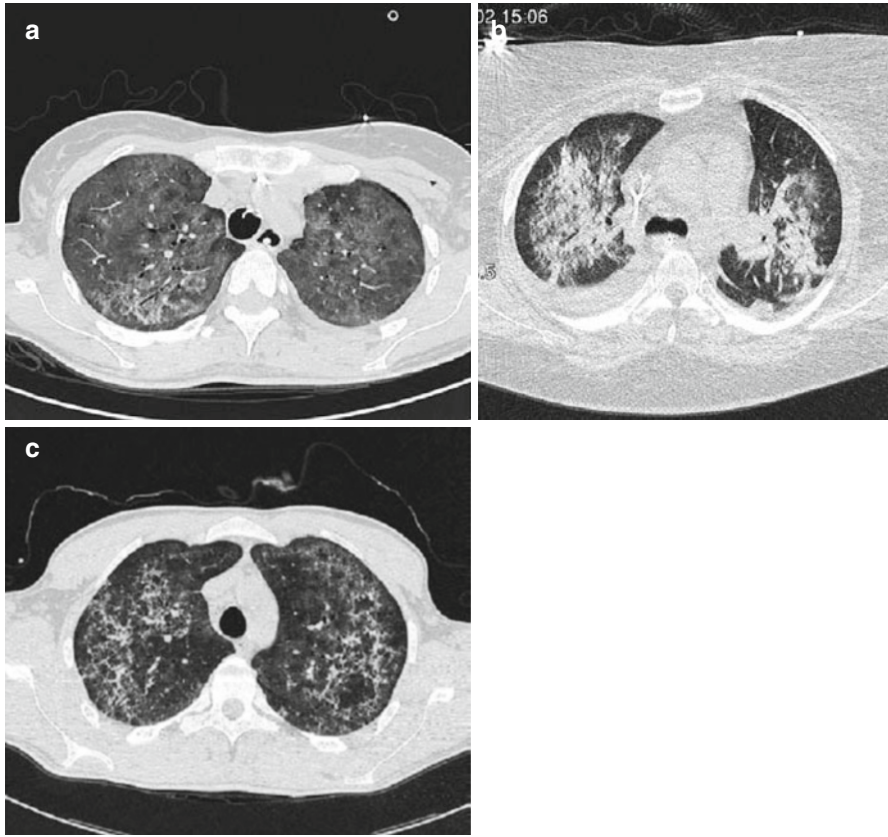
Fig. 7.9 Bilateral pneumonia caused by *Pneumocystis jiroveci* at different stages of immunosuppression. The subpleural space is typically spared out. Diffuse ground-glass opacification appears typically in the early phase of infection (**a**), while consolidations appear during a fulminant course (**b**). The predominance of intralobular linear patterns becomes visible during a later stage of PcP and under antimicrobial treatment (**c**)

of ground-glass opacities and intralobular septae sparing out the subpleural space (i.e., perihilar distribution) is very typical for PcP (Fig. 7.9) [33, 39, 40].

7.3.4   Lung Tuberculosis

Tuberculosis (TB) has to be considered as a rare but relevant differential diagnosis. In immunocompromised hosts, TB appears different compared to immunocompetent hosts (e.g., gangliopulmonary (primary) forms) [41]. More widespread lymphogenic and hematogenous dissemination can occur, and therefore, the clinical course might be fulminant [41, 42]. On the other hand, TB might mimic or come along with other infections like pulmonary aspergillosis or systemic candidiasis [42].
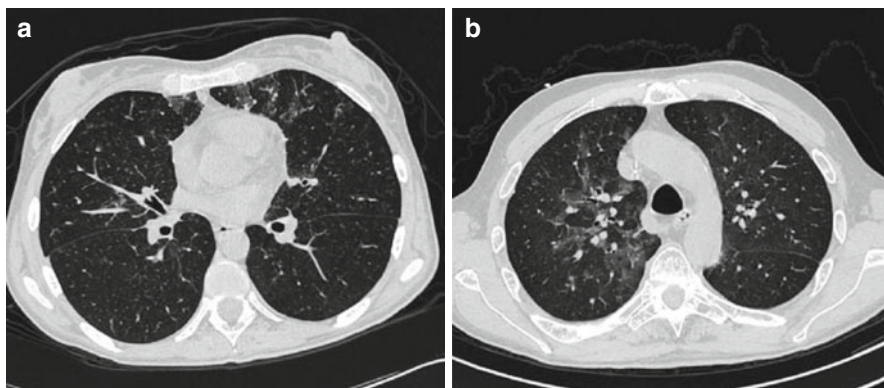
Fig. 7.10 Bilateral ground-glass opacification and mosaic pattern in both patients. However, pneumonia in patient A is caused by cytomegalovirus (*CMV*), and patient B by respiratory syncytial virus (*RSV*). Note the mosaic pattern resulting from affected and non-affected secondary lobules lying adjacent to one another

In immunocompromised hosts a segmental bronchial spread (resulting in a "tree-in-bud" sign) of small, sometimes, cavitated ill-defined nodules can be obtained as well as a miliar distribution [41, 42]. Gangliopulmonary (primary) forms, however, present with nonhomogenous consolidation and necrotizing mediastinal or hilar lymphadenopathy [41].

7.3.5   Viral Pneumonia

Interstitial pneumonia caused by viral infection may occur primarily in aSCT recipients but also in neutropenic and T-cell-immunosuppressed patients. Mortality rate may be up to 50 %. Most frequently, cytomegalovirus (CMV) is suspected; however, other herpesviruses, influenza, parainfluenza, adenovirus, or respiratory syncytial (RSV) viruses have to be considered as well. There are no specific radiological patterns available to differentiate various forms of viral pneumonia. However, confirming the suspicion of a viral pneumonia may be a clinically useful information, since effective drugs are available for some of these viruses. The typical appearance of viral pneumonia in the early stage is ground-glass opacification [33] and a mosaic pattern with affected and non-affected secondary lobules lying adjacent to one another (Fig. 7.10).

7.3.6   Noninfectious Pulmonary Lesions

Certain noninfectious diseases have to be considered in hematological patients: graft-versus-host disease (GVHD), radiation or drug toxicity, pulmonary congestion, bleeding, or progressive underlying malignancy. Fever, dyspnea, or clinical chemistry findings (c-reactive protein, elevation of liver function tests) might be

Fig. 7.11 A 28-year-old male after allogeneic retransplantation. HRCT was performed due to fever, cough, and dyspnea. Peripheral intralobular septae (*arrow*) and ground-glass opacification were seen on day 91 posttransplant. Tree-in-bud pattern (*arrowhead*) points at bronchiolitis obliterans. Acute GVHD was diagnosed from transbronchial biopsy. Under appropriate immunosuppression, clinical symptoms and radiological signs disappeared. Note the similarity to Fig. 7.13

caused by some of these processes and obscure the differentiation from infection. CT may help to detect and discriminate these diseases [6, 7, 18, 32].

7.3.7   Graft-Versus-Host Disease

Pulmonary manifestation of chronic GVHD occurs in approximately 10 % of patients after allogeneic hematopoietic stem cell transplantation (Fig. 7.11) [43]. Bronchiolitis obliterans is the pulmonary manifestation of this rejection [28]. The radiological appearance is similar to viral pneumonia, and clinical appearance and time point for both diseases are often similar (Fig. 7.11).

Ground-glass opacification and mosaic pattern, as well as signs of bronchiolitis obliterans such as air-trapping [24, 28] and bronchus wall thickening, occur during the early stage of pulmonary GVHD (Fig. 7.11), whereas intralobular septae and tree-in-bud sign follow in later stages [7, 43, 44].

7.3.8   Radiation Toxicity

An incidence of 5–25 % pulmonary radiogenic toxicity even after total body irradiation (TBI) applied for conditioning prior to stem cell transplantation is reported

Fig. 7.12 Three weeks after radiation therapy for malignant spine destruction, this patient suffered from fever and dyspnea. Perihilar infiltrates appeared suddenly. Intralobular septae, consolidation, and ground-glass opacification were visible on HRCT. Especially the paramediastinal distribution of the infiltrates led to the differential diagnosis of radiation pneumonitis. After failure of antibiotic treatment, steroids were applied, resulting in improvement of symptoms and reduction of infiltrates

[45]. It emerges approximately 3 weeks after exposure but can also occur several months later [44, 45].

On CT scans, radiation-induced toxicity is characterized by ground-glass opacities with transition to consolidations (Fig. 7.12) [44, 45]. The key finding is the limitation of these patterns to the exposed parenchyma. For TBI, lungs are shielded, while paramediastinal and apical lung parenchyma is affected from radiation. Of note, demarcation of initially exposed from nonexposed lung parenchyma is blurred frequently due to deformation of lung parenchyma and to bridle.

7.3.9 Drug Toxicity

Chemotherapy protocols may lead to pulmonary toxicity. Some of the frequently used agents are bleomycin, high-dose methotrexate (MTX) or cytarabine (Ara-C), or carmustine (BCNU) (Fig. 7.13) [46]. Radiologists should be informed of previous exposure of patients to these agents when evaluating CT scans for pulmonary abnormalities.

Fig. 7.13 A 40-year-old male who received chemotherapy including bleomycin for testicular cancer and had fever, cough, and dyspnea. CT revealed peripheral intralobular septae and ground-glass opacification (**a**). Bleomycin toxicity was suspected and histologically confirmed. Symptoms disappeared and findings decreased after application of steroids. Note the similarity to Fig. 7.11
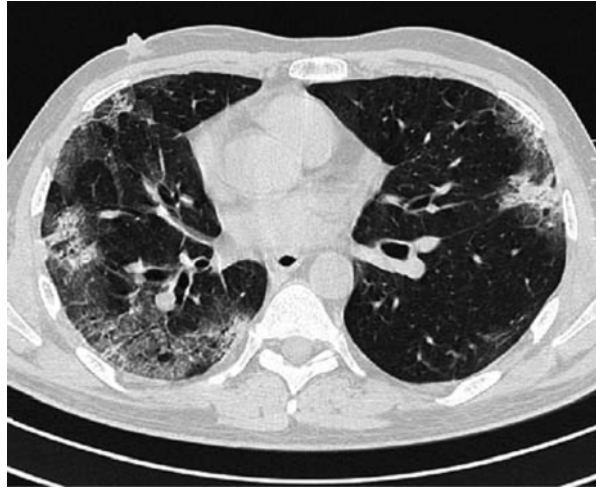
The term "drug-induced pneumonitis" includes mainly nonspecific interstitial pneumonia (NSIP) and cryptogenic organizing pneumonia (COP, formerly known as bronchiolitis obliterans organizing pneumonia, BOOP) [46]. The CT appearance of NSIP consists of ground-glass opacities with transition to consolidations, intralobular septae, traction bronchiectasis, air-trapping, and in a later phase the nonspecific "crazy-paving" pattern [44, 46]. This is quite similar to radiation toxicity but without being limited to the radiation field.

7.3.10 Pulmonary Congestion

Dyspnea and infiltration are frequent in patients suffering from pulmonary congestion. Extensive hydration for renal protection during chemotherapy or to overcome renal impairment may cause pulmonary congestion also in younger patients. It is one of the most frequent disorders in patients undergoing intensive care.

At CXR, pulmonary congestion might be combined with infiltration. CT shows thickening of lymphatic vessels, corresponding to classical "Kerley lines" on conventional chest radiographs (Fig. 7.14).

7.3.11 Leukemic Infiltrates

Leukemic pulmonary infiltration is a less common clinical finding. Especially the perilymphatic pulmonary interstitium is involved [47]. This can be visualized on CT scans as thickening of bronchovascular bundles and interlobular septae. Besides

Fig. 7.14 Thickening of the intralobular septae resulting from fluid overload in lymphatic vessels

this, non-lobular and non-segmental ground-glass opacifications can be seen [32]. This pattern arrangement might mimic pulmonary congestion (Fig. 7.14).

7.3.12 Pulmonary Hemorrhage

In pancytopenia, pulmonary bleeding may occur spontaneously, secondary to invasive infections, after interventions (e.g., bronchoscopy and BAL), or during marrow recovery particularly in patients with fungal pneumonia [27].

Pulmonary bleeding might cause a focal or diffuse pattern, and the phenomenon of sedimentation within the secondary lobules can sometimes be depicted for few days (Fig. 7.15).

7.4 Extrapulmonary Focus

7.4.1 Liver and Spleen

Suspicious clinical symptoms or unexplained laboratory findings may suggest an involvement of the liver and spleen [13], particularly secondary to fungemia [54]. In addition to candidiasis, also mycobacteriosis, bacterial granulomatous hepatitis, viral hepatitis, and noninfectious organ involvement such as drug-related hepatotoxicity, GVHD, veno-occlusive disease (VOD), or relapse of the underlying disease have to be considered [12].

Fig. 7.15 The bilateral ground-glass opacification has an anterior-to-posterior gradient (1) over the whole lung and (2) within certain secondary lobules. This gravity-dependent sedimentation phenomenon can also occur temporarily and may be localized, e.g., after bronchoscopy and BAL

7.4.2 Gastrointestinal

Due to its microbial flora and the chemotherapy-induced mucosal injury, the gastrointestinal tract is particularly exposed to infection. However, without any history of surgical intervention, gastrointestinal involvement is rare. The main affections of the gastrointestinal tract, such as CMV colitis, pseudomembranous enterocolitis, enterocolitis in the context of rejection (GVHD), appendicitis, and diverticulitis, can be seen in CT as bowel wall thickening even without intravenous contrast after adequate oral, rectal contrast application [55].

7.4.3 Brain

Cerebral infection is a rare complication of myelosuppressive chemotherapy. It is more likely in the aSCT setting than after conventional chemotherapy [2]. Besides infectious diseases (e.g., herpesvirus group, toxoplasmosis, aspergillosis, mucormycosis, listeriosis), diagnoses such as bleeding, ischemia, drug toxicity (cyclosporine, ribavirin, voriconazole, etc.), and electrolyte disorders have to be taken into consideration. CT is helpful in emergency situations, while MRI is the method of choice in brain imaging in terms of sensitivity and specificity for detection and characterization of brain abnormalities [12].

7.4.4   Paranasal Sinuses

Since the sinuses are part of the respiratory tract, there is a coincidence of pneumonia [56]. Since the risk for sinusitis is up to 30 % in allogeneic stem cell transplant recipients, paranasal sinuses are often screened by CT prior to transplantation [57]. Bone erosion and orbital or brain invasion are classified by the 2008 EORTC guideline as clinical criteria for probable invasive fungal disease [51].

References

1. Chanock S. Evolving risk factors for infectious complications of cancer. Hematol Oncol Clin North Am. 1993;7:771–93.
2. Hiddemann W, Maschmeyer G, Runde V, Einsele H. Prevention, diagnosis and therapy of infections in patients with malignant diseases. Internist. 1996;37:1212–24.
3. Pizzo PA, Robichaud KJ, Gill FA, Witebsky FG. Empiric antibiotic and antifungal therapy for cancer patients with prolonged fever and granulocytopenia. Am J Med. 1982;72:101–11.
4. Maschmeyer G, Link H, Hiddemann W, Meyer P, Helmerking M, Eisenmann E, Schmitt J, Adam D. Pulmonary infiltrations in febrile neutropenic patients. Risk factors and outcome under empirical antimicrobial therapy in a randomized multicenter trial. Cancer. 1994;73: 2296–304.
5. Maschmeyer G. Pneumonia in febrile neutropenic patients: radiologic diagnosis. Curr Opin Oncol. 2001;13:229–35.
6. Schaefer-Prokop C, Prokop M, Fleischmann D, Herold C. High-resolution CT of diffuse interstitial lung disease: key findings in common disorders. Eur Radiol. 2001;11:373–92.
7. Tanaka N, Matsumoto T, Miura G, Emoto T, Matsunaga N. HRCT findings of chest complications in patients with leukemia. Eur Radiol. 2002;12:1512–22.
8. Einsele H, Bertz H, Beyer J, Kiehl MG, Runde V, Kolb H-J, Holler E, Beck R, Schwertfeger R, Schumacher U, Hebart H, Martin H, Kienast J, Ullmann AJ, Maschmeyer G, Krüger W, Link H, Schmidt CA, Oettle H, Klingebiel T. Epidemiologie und interventionelle Therapiestrategien infektiöser Komplikationen nach allogener Stammzelltransplantation. Dtsch Med Wochenschr. 2001;126:1278–84.
9. Maschmeyer G, Buchheidt D, Einsele H, Heußel CP, Holler E, Lorenz J, Schweigert M. Diagnostik und Therapie von Lungeninfiltraten bei febrilen neutropenischen Patienten – Leitlinien der Arbeitsgemeinschaft Infektionen in der Hämatologie und Onkologie der Deutschen Gesellschaft für Hämatologie und Onkologie. Dtsch Med Wochenschr. 1999;9:124(Suppl 1):S18–23. Update: http://www.dgho-infektionen.de/agiho/content/e125/e670/lugeninfiltrate.pdf. 26.03.03.
10. Ascioglu S, Rex JH, de Pauw B, Bennett JE, Bille J, Crokaert F, Denning DW, Donnelly JP, Edwards JE, Erjavec Z, Fiere D, Lortholary O, Maertens J, Meis JF, Patterson TF, Ritter J, Selleslag D, Shah PM, Stevens DA, Walsh TJ. Defining opportunistic invasive fungal infections in immunocompromised patients with cancer and hematopoietic stem cell transplants: an international consensus. Clin Infect Dis. 2002;34:7–14.
11. Edinburgh KJ, Jasmer RM, Huang L, Reddy GP, Chung MH, Thompson A, Halvorsen Jr RA, Webb RA. Multiple pulmonary nodules in AIDS: usefulness of CT in distinguishing among potential causes. Radiology. 2000;214:427–32.
12. Heussel CP, Kauczor H-U, Heussel G, Poguntke M, Schadmand-Fischer S, Mildenberger P, Thelen M. Magnetic resonance imaging (MRI) of liver and brain in hematologic-oncologic patients with fever of unknown origin. Rofo. 1998;169:128–34.
13. Heußel CP, Kauczor H-U, Heußel G, Derigs HG, Thelen M. Looking for the cause in neutropenic fever. Imaging diagnostics. Radiologe. 2000;40:88–101.

14. Azoulay E, Darmon M, Delclaux C, Fieux F, Bornstain C, Moreau D, Attalah H, Le Gall JR, Schlemmer B. Deterioration of previous acute lung injury during neutropenia recovery. Crit Care Med. 2002;30:781–6.
15. Navigante AH, Cerchietti LC, Costantini P, Salgado H, Castro MA, Lutteral MA, Cabalar ME. Conventional chest radiography in the initial assessment of adult cancer patients with fever and neutropenia. Cancer Control. 2002;9:346–51.
16. Barloon TJ, Galvin JR, Mori M, Stanford W, Gingrich RD. High-resolution ultrafast chest CT in the clinical management of febrile bone marrow transplant patients with normal or nonspecific chest roentgenograms. Chest. 1991;99:928–33.
17. Weber C, Maas R, Steiner P, Kramer J, Bumann D, Zander AR, Bucheler E. Importance of digital thoracic radiography in the diagnosis of pulmonary infiltrates in patients with bone marrow transplantation during aplasia. Rofo. 1999;171:294–301.
18. McLoud TC, Naidich DP. Thoracic disease in the immunocompromised patient. Radiol Clin North Am. 1992;30:525–54.
19. Cardillo I, Boal TJ, Einsiedel PF. Patient doses from chest radiography in Victoria. Australas Phys Eng Sci Med. 1997;20:92–101.
20. Schöpf UJ, Becker CXR, Obuchowski NA, Rust G-F, Ohnesorge BM, Kohl G, Schaller S, Modic MT, Reiser MF. Multi-slice computed tomography as a screening tool for colon cancer, lung cancer and coronary artery disease. Eur Radiol. 2001;11:1975–85.
21. Heussel CP, Kauczor H-U, Heussel G, Fischer B, Begrich M, Mildenberger P, Thelen M. Pneumonia in febrile neutropenic patients, bone-marrow and blood stem-cell recipients: use of high-resolution CT. J Clin Oncol. 1999;17:796–805.
22. Remy-Jardin M, Giraud F, Remy J, Copin MC, Gosselin B, Duhamel A. Computed tomography assessment of ground-glass opacity: semiology and significance. J Thorac Imaging. 1993;8:249–64.
23. Kauczor HU, Schnuetgen M, Fischer B, et al. Pulmonary manifestations in HIV patients: the role of chest films, CT and HRCT. Rofo. 1995;162:282–7.
24. Grenier PA, Beigelman-Aubry C, Fetita C, Preteux F, Brauner MW, Lenoir S. New frontiers in CT imaging of airway disease. Eur Radiol. 2002;12:1022–44.
25. Flohr T, Stierstorfer K, Bruder H, Simon J, Schaller S. New technical developments in multislice CT – part 1: approaching isotropic resolution with sub-millimeter 16-slice scanning. Rofo. 2002;174:839–45.
26. Eibel R, Ostermann H, Schiel X. Thorakale Computertomographie von Lungeninfiltraten. http://www.dgho-infektionen.de/agiho/content/e134/e619/e657. 26.03.03.
27. Heussel CP, Kauczor HU, Heussel G, Mildenberger P, Dueber C. Aneurysms complicating inflammatory diseases in immunocompromised hosts: value of contrast-enhanced CT. Eur Radiol. 1997;7:316–9.
28. Conces DJ. Noninfectious lung disease in immunocompromised patients. J Thorac Imaging. 1999;14:9–24.
29. Leutner CC, Gieseke J, Lutterbey G, Kuhl CK, Glasmacher A, Wardelmann E, Theisen A, Schild HH. MR imaging of pneumonia in immunocompromised patients: comparison with helical CT. AJR Am J Roentgenol. 2000;175:391–7.
30. Leutner C, Schild H. MRI of the lung parenchyma. Rofo. 2001;173:168–75.
31. Caillot D, Couaillier JF, Bernard A, Casasnovas O, Denning DW, Mannone L, Lopez J, Couillault G, Piard F, Vagner O, Guy H. Increasing volume and changing characteristics of invasive pulmonary aspergillosis on sequential thoracic computed tomography scans in patients with neutropenia. J Clin Oncol. 2001;19:253–9.
32. Tanaka N, Matsumoto T, Miura G, Emoto T, Matsunaga N, Satoh Y, Oka Y. CT findings of leukemic pulmonary infiltration with pathologic correlation. Eur Radiol. 2002;12: 166–74.
33. Reittner P, Ward S, Heyneman L, Johkoh T, Müller NL. Pneumonia: high-resolution CT findings in 114 patients. Eur Radiol. 2003;13:515–21.
34. Conces DJ. Bacterial pneumonia in immunocompromised patients. J Thorac Imaging. 1998;13:261–70.

35. Heußel CP, Ullmann AJ, Kauczor H-U. Fungal pneumonia. Radiologe. 2000;40:518–29.
36. Kim MJ, Lee KS, Kim J, Jung KJ, Lee HG, Kim TS. Crescent sign in invasive pulmonary aspergillosis: frequency and related CT and clinical factors. J Comput Assist Tomogr. 2001;25: 305–10.
37. Kim K, Lee MH, Kim J, Lee KS, Kim SM, Jung MP, Han J, Sung KW, Kim WS, Jung CW, Yoon SS, Im YH, Kang WK, Park K, Park CH. Importance of open lung biopsy in the diagnosis of invasive pulmonary aspergillosis in patients with hematologic malignancies. Am J Hematol. 2002;71:75–9.
38. Stringer JR, Beard CB, Miller RF, Wakefield AE. A new name (Pneumocystis jiroveci) for Pneumocystis from humans. Emerg Infect Dis. 2002. http://www.cdc.gov/ncidod/EID/vol8no9/02-0096.htm. 26.03.03.
39. Hidalgo A, Falcó V, Mauleón S, Andreu J, Crespo M, Ribera E, Pahissa A, Cáceres J. Accuracy of high-resolution CT in distinguishing between Pneumocystis carinii pneumonia and non-Pneumocystis carinii pneumonia in AIDS patients. Eur Radiol. 2003. doi:10.1007/s00330-002-1641-6.
40. McGuinness G, Gruden JF. Viral and pneumocystis carinii infections of the lung in the immunocompromised host. J Thorac Imaging. 1999;14:25–36.
41. Van Dyck P, Vanhoenacker FM, Van den Brande P, De Schepper AM. Imaging of pulmonary tuberculosis. Eur Radiol. 2003. doi:10.1007/s00330-002-1612-y.
42. Goo JM, Im JG. CT of tuberculosis and nontuberculous mycobacterial infections. Radiol Clin North Am. 2002;40:73–87.
43. Leblond V, Zouabi H, Sutton L, Guillon JM, Mayaud CM, Similowski T, Beigelman C, Autran B. Late CD8+ lymphocytic alveolitis after allogeneic bone marrow transplantation and chronic graft-versus-host disease. Am J Respir Crit Care Med. 1994;150:1056–61.
44. Oikonomou A, Hansell DM. Organizing pneumonia: the many morphological faces. Eur Radiol. 2002;12:1486–96.
45. Monson JM, Stark P, Reilly JJ, Sugarbaker DJ, Strauss GM, Swanson SJ, Decamp MM, Mentzer SJ, Baldini EH. Clinical radiation pneumonitis and radiographic changes after thoracic radiation therapy for lung carcinoma. Cancer. 1998;82:842–50.
46. Erasmus JJ, McAdams HP, Rossi SE. High-resolution CT of drug-induced lung disease. Radiol Clin North Am. 2002;40:61–72.
47. Heyneman LE, Johkoh T, Ward S, Honda O, Yoshida S, Muller NL. Pulmonary leukemic infiltrates: high-resolution CT findings in 10 patients. AJR Am J Roentgenol. 2000;174: 517–21.
48. Morrell M, Fraser VJ, Kollef MH. Delaying the empiric treatment of candida bloodstream infection until positive blood culture results are obtained: a potential risk factor for hospital mortality. Antimicrob Agents Chemother. 2005;49:3640–5.
49. Gefter WB, Albelda S, Talbot G, Gerson S, Cassileth P, Miller WT. New observations on the significance of the air crescent in invasive pulmonary aspergillosis. Radiology. 1984;153:136.
50. Kuhlman JE, Fishman EK, Siegelman SS. Invasive pulmonary aspergillosis in acute leukemia: characteristic findings on CT, the CT halo sign, and the role of CT in early diagnosis. Radiology. 1985;157:611–4.
51. De Pauw B, Walsh TJ, Donnelly JP, Stevens DA, Edwards JE, Calandra T, Pappas PG, Maertens J, Lortholary O, Kauffman CA, Denning DW, Patterson TF, Maschmeyer G, Bille J, Dismukes WE, Herbrecht R, Hope WW, Kibbler CC, Kullberg BJ, Marr KA, Muñoz P, Odds FC, Perfect JR, Restrepo A, Ruhnke M, Segal BH, Sobel JD, Sorrell TC, Viscoli C, Wingard JR, Zaoutis T, Bennett JE, European Organization for Research and Treatment of Cancer/Invasive Fungal Infections Cooperative Group; National Institute of Allergy and Infectious Diseases Mycoses Study Group (EORTC/MSG) Consensus Group. Revised definitions of invasive fungal disease from the European Organization for Research and Treatment of Cancer/Invasive Fungal Infections Cooperative Group and the National Institute of Allergy and

Infectious Diseases Mycoses Study Group (EORTC/MSG) Consensus Group. Clin Infect Dis. 2008;46:1813–21.

52. Greene RE, Schlamm HT, Oestmann JW, Stark P, Durand C, Lortholary O, Wingard JR, Herbrecht R, Ribaud P, Patterson TF, Troke PF, Denning DW, Bennett JE, de Pauw BE, Rubin RH. Imaging findings in acute invasive pulmonary aspergillosis: clinical significance of the halo sign. Clin Infect Dis. 2007;44:373–9.
53. Eibel R, Herzog P, Dietrich O, Rieger CT, Ostermann H, Reiser MF, Schoenberg SO. Pulmonary abnormalities in immunocompromised patients: comparative detection with parallel acquisition MR imaging and thin-section helical CT. Radiology. 2006;241:880–91.
54. Anttila VJ, Ruutu P, Bondestam S, et al. Hepatosplenic yeast infection in patients with acute leukemia: a diagnostic problem. Clin Infect Dis. 1994;18:979–81.
55. Donnelly LF, Morris CL. Acute graft-versushost disease in children: abdominal CT findings. Radiology. 1996;199:265–8.
56. Savage DG, Taylor P, Blackwell J, et al. Paranasal sinusitis following allogeneic bone marrow transplant. Bone Marrow Transplant. 1997;19:55–9.
57. Oberholzer K, Kauczor H-U, Heußel CP, Derigs HG, Thelen M. Klinische Relevanz der NNH-CT vor Knochenmarktransplantation. Rofo. 1997;166:493–7.
58. Cornely OA, Maertens J, Bresnik M, Ullmann AJ, Ebrahimi R, Herbrecht R. Treatment outcome of invasive mould disease after sequential exposure to azoles and liposomal amphotericin B. J Antimicrob Chemother. 2010;65(1):114–7.